Journal of the European Ceramic Society 20 (2000) 517–526

The rate-determining mechanism in the sintering of undoped nonstoichiometric barium titanate

Ming-Hong Lin [a,*], Jung-Fang Chou [b], Hong-Yang Lu [a]

[a] *Institute of Materials Science and Engineering, National Sun Yat-Sen University, Kaohsiung 80424, Taiwan*
[b] *Department of Electrical Engineering, Kung-Shan Institute of Technology, Yung-Kang, Tainan 710, Taiwan*

Received 30 March 1999; received in revised form 21 June 1999; accepted 28 June 1999

Abstract

High-purity undoped nonstoichiometric $BaTiO_3$ powder of TiO_2-excess and BaO-excess has been pressureless-sintered in the range of 1215–1340°C using conventional tube furnace. Low temperature sintering of the TiO_2-excess composition results in the characteristic plate-like grains grown along the {111} plane. Surface energy anisotropy is proposed to account for the anomalous microstructural development and low final sintered density. The activation enthalpy values (ΔH) deduced from isothermal sintering are 522 ± 130 and 396 ± 16 kJ mol for the TiO_2-excess and BaO-excess composition, respectively. The rate-determining mechanism for the solid-state sintering of the undoped nonstoichiometric $BaTiO_3$ powder is discussed.

Keywords: $BaTiO_3$; Microstructure-final; Perovskites; Sintering

1. Introduction

Stoichiometric $BaTiO_3$ powder of high purity is practically unavailable from commercial sources. Most of it is nonstoichiometric[1] containing various levels of impurities, notably of SrO, CaO, SiO_2 and Al_2O_3. The nonstoichiometry was usually taken to account for the inconsistency in the sintering of "pure" $BaTiO_3$ powder in the literature. The traditional wisdom has been that the TiO_2-excess compositions enhance while the BaO-excess hinder the sintering of $BaTiO_3$.[2,3]

Sintering studies of $BaTiO_3$ has often been inconclusive[1,4] in terms of the rate-determining mechanism for densification. In solid-state sintering, it includes both the diffusion species and the diffusion path still remains controversial. Major difficulties arise from two fundamental aspects. Firstly, it is associated with the lowest liquid eutectic temperature of $BaTiO_3$–$Ba_6Ti_{17}O_{40}$ at $\sim$ 1332°C in the BaO–TiO_2 system.[5] Above this, the densification assisted by the eutectic liquid phase easily overwhelms that in the solid state. It is particularly pronounced for the TiO_2-excess compositions in which $Ba_6Ti_{17}O_{40}$ is formed by solid-state reaction[6] upon heating samples to the desired sintering temperatures. The trace impurities contained in the initial powders may also decrease the liquid formation temperature of Al_2O_3–SiO_2–TiO_2 further down to $\sim$ 1250°C.[7] The use of high sintering temperatures adopting the idea of fast-firing is also not suitable, not only because of the 1332°C eutectic but also the cubic $\rightarrow$ hexagonal phase transformation occurs at 1430–1460°C.[5] The applicable temperature range for the study of solid-state sintering of $BaTiO_3$ compositions is therefore limited[4] to $<$1250°C. Choosing low temperature sintering to avoid the liquid eutectics, however, has often been compounded by the formation of plate-like grains faceted along {111}.[8]

Secondly, the activation enthalpy (ΔH) values, derived from different techniques concerning cation and oxygen diffusion in $BaTiO_3$ listed in Table 1, are very scattered. Data from sintering and creep studies are not conclusive.[1,4,14] It is partly because of the various experimental techniques adopted by individual research, and partly the multiple mechanisms that occur concurrently during entering. Those values deduced from the studies of hot-pressing[1,4] and isothermal pressureless-sintering[14] fall into a considerable range of 290 $\sim$ 588 kJ/mol. Interface-reaction-controlled liquid-phase

* Corresponding author at present address: Department of Mechanical Engineering, National Kaohsiung Institute of Technology, Kaohsiung 80782, Taiwan.

0955-2219/00/$ - see front matter
PII: S0955-2219(99)00174-0

Table 1
Activation enthaply values for $BaTiO_3$

Diffusion element	ΔH (kJ mol^{-1})	Temperature range (°C)	Experimental method	Reference
Ba	372	884–1180	Self-diffusion	9
	332.9		Theoretical calculation	10
	226		Defect-chemistry model	11
O	469	700–1000	Sintering model	12
	53	900-1100	Self-diffusion	9
	59.6		Theoretical calculation	10
	197		Defect-chemistry model	11
	42.5		Trace	13
Ti	293		Self-diffusion	9
	1458		Theoretical calculation	10
Undefined	506	1260–1400	Creep model	1
	336–588		Sintering model	14
	400	1060–1200	Creep model	4

sintering mechanism[1] and grain-diffusion of the Coble creep in solid-state sintering[4] were proposed from the respective hot-pressing kinetics results where temperatures on both sides of the lowest eutectic of $\sim$ 1332°C in the BaO–TiO_2 system had been experimented. Hyper-stoichiometric TiO_2-excess compositions were often adopted in their studies.[1,4,14] Comparing the ΔH values derived from the sintering models[1,4,14] with data from other techniques, it would appear that Ba^{2+}-ion is the rate-determining species in the solid-state. However, whether any liquid eutectic phase was involved in the sintering is not known for certain, particularly with low temperature sintering. The rate-determining mechanism in the solid-state sintering of $BaTiO_3$ remains ambiguous before careful microstructural analysis.

Thermodynamically, the formation of one titanium vacancy in its intrinsic defect regime appears to be energetically more favourable[10] than two barium vacancies in the undoped $BaTiO_3$, regardless of the discrepancy in the actual formation energy values.[15] is More recent study of the PTCR $BaTiO_3$ ceramics suggested[16] that Ti^{4+}-ion is the rate-determining species for the solid-state sintering of Nb_2O_5-donor-doped compositions. It was also implied that titanium vacancy ($V_{Ti}^{''''}$) is the principal charge compensating defect Ti for the substitutional defect $Nb_{Ti}^{\bullet}$ of positive effect charge, and so the energetically more favourable defect species in donor-doped compositions. However, Chiang et al.,[17] accepting that titanium vacancy may be the thermodynamically more favourable defect species, has proposed that barium vacancy (V_{Ba}'') predominates in a metastable defect equilibrium controlled by kinetic factor. Transition of the principal charge compensation mechanism from barium to titanium vacancy upon increasing Nb_2O_5 donor-level was also reported.[18] is Nevertheless, solid-state sintering has usually been assumed without further confirmation of the absence of liquid-phase by appropriate microstructural observations.

We have investigated the sintering kinetics of undoped TiO_2-excess and BaO-excess $BaTiO_3$ compositions using a conventional tube furnace. Sintering behaviour is reported when the rate-determining mechanism is proposed. Microstructure analysis of the sintered samples has also been emphasised in order to support the sintering mechanism derived from the kinetic results.

2. Experimental procedure

Commercial $BaTiO_3$ powder (Ticon® HPB) supplied by TAM Ceramics (Niagara Falls, NY) was used in this study. Two nonstoichiometric compositions of Ba/Ti = 0.997 TiO_2-excess and 1.013 BaO-excess were chosen. The initial powder was mixed with 1 wt% PVB (polyvinyl butyral) binder in absolute alcohol before milling in a polyurethane (PU) jar with PU-coated steel balls for 2 h. It was dried subsequently at 100°C for $>$12 h. After being deagglomerated by using agate mortar and pestle and passed through $\sim$74 μm mesh, an appropriate amount of powder was dry-pressed to 10 mm diameter and $\sim$0.5 mm thick in a WC-inserted steel die by applying a unaxial pressure of 100 MPa. It was then sintered in a conventional tube furnace at the desired temperatures. For fast-firing in conventional furnaces, samples were pushed into the hot zone within 3 min using a stainless steel wire, which has enabled a high heating rate of $\sim$ 400°C/min. These samples were used to establish the isothermal sintering curves in order that microstructural change during heating-up stage can be minimised. For constant heating-rate (CHR) sintering, 2.5, 50, 20 and 40°C/min were adopted. The sintered density was determined by applying Archimedes technique when distilled water was used as the immersion medium. The average grain size was determined by measuring more than 200 grains adopting $G_{av} = kL$, where L = average lineal intercept.[15] The constant k is taken as 1.56 for grains of the tetrakaidecahedral shape. Sintering kinetic curves are established by plotting final sintered density for various sintering time. The densification rate at any sintered density was obtained by differentiating the sintering kinetic curves using Kaleidagraph® software in a Macintosh® computer.

Crystalline phases were identified by X-ray diffractometry (XRD, Siemens D5000, Karlschrule, Germany) using CuK_α radiation operating at 30 kV/2 mA with Ni filter. The sintered samples were mechanically ground and polished with SiC grits successively before diamond lapping to 1 μm roughness for microstructural observations. Both a reflected light optical microscope

and scanning electron microscope (SEM, JEOL 6400, Tokyo, Japan) were used on polished sections. Grain-boundaries were delineated by thermal etching at 200°C below the sintering temperatures, or chemical etching using 1%HF solution where appropriate. Thin foils for transmission electron microscopy (TEM) were prepared by slicing as-sintered samples to ~ 200 μm thickness, ultrasonic cutting to 3 mm (ϕ) discs, mechanical polishing to 1 μm roughness and ~30 μm thickness, dimple-grinding and Ar^+-ion beam thinning to electron transparency. Observations were performed in JEOL 200CX and AEM3010 operating at 200 and 300 kV, respectively.

3. Results

3.1. Sintering kinetics

The kinetic curves of pressureless-sintering for both the TiO_2-excess and BaO-excess compositions when sintered at 1215°C are presented in Fig. 1. An immediate observation is that the sintered density of the TiO_2-excess composition is always lower than that of the BaO-excess up to a sintering period of 150 h. The BaO-excess powder was better sintered with a final density of $\rho_{rel} \approx 97.5\%$ (vs 83% of the TiO_2-excess) below the lowest eutectic temperature of 1250°C. Possible liquid eutectic phase is associated with 20 trace impurities of the composition Al_2O_3–SiO_2–TiO_2,[20] or that consisting of the aluminosilicates.[1] A discrepancy of $\Delta\rho_{rel} = 15\%$ also indicates that the TiO_2-excess composition is still in the intermediate sintering stage while the BaO-excess has reached its final stage.

Pressureless-sintering kinetic results of both the TiO_2-excess and BaO-excess compositions for 1250–1310°C are presented in Fig. 2(a) and (b), respectively. The increment of sintered density with temperature become more appreciable progressively from 1250 to 1310°C for the TiO_2-excess composition. The change from 1215 to 1250°C is most conspicuous indicating enhanced densification by a liquid phase. Apart from the $A1_2O_3$–SiO_2–TiO_2 eutectic liquid[20] for TiO_2-excess samples, the increased densification in both compositions can also be attributed to the liquid eutectics at ~ 1245–1260°C in the $BaTiO_3$–SiO_2 system[21] when SiO_2 is present in the initial powder. A similar increment is also detected for the BaO-excess samples, but not as considerable. Final sintered densities obtained for the BaO-excess powder are in the range of $\rho_{rel} = 94 \sim 97\%$ with a deviation much smaller than $\rho_{rel} = 85 \sim 96\%$ of the TiO_2-excess samples. The indication is if the sintering of the BaO-excess composition is assisted by liquid eutectics at all, it would be of completely different chemistry from that involved in the TiO_2-excess samples.

The Arrhenius plots of $\ln[(d\rho/dt)(dT/dt)(T)]$ vs $(1/T)$ for both compositions sintered by constant-heating-rate technique are given in Fig. 3(a) and (b). Data of the densification rate are taken from relative densities of greater than 75% where the contribution of particle rearrangement to densification is considered negligible.

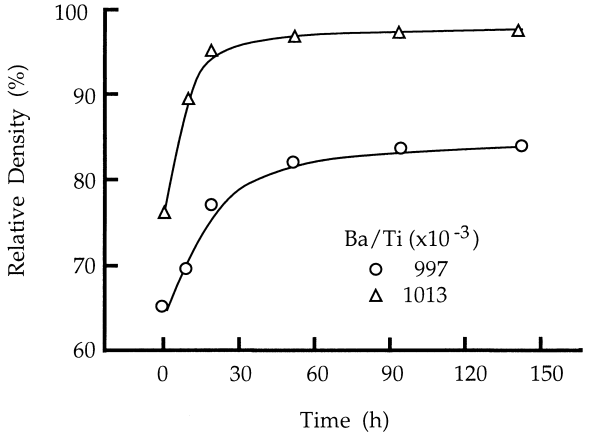

Fig. 1. Pressureless-sintering kinetic curves at 1215°C for TiO_2 excess and BaO-excess $BaTiO_3$ composition.

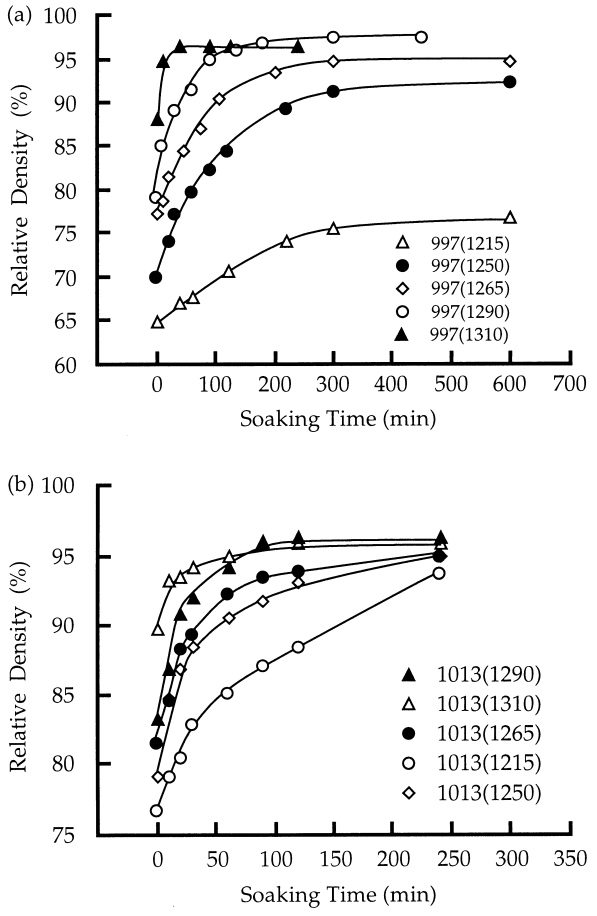

Fig. 2. Pressureless-sintering kinetic curves for (a) TiO_2-excess and (b) BaO-excess $BaTiO_3$ composition sintered at 1215, 1250, 1265, 1290 and 1310°C.

For the BaO-excess composition [Fig. 3(b)], the ΔH-values derived from CHR are 1168 ± 186 kJ/mol which is relatively large in comparison with those given in Table 1. Difficulties have occurred when constructing similar plots for the TiO_2-excess composition. Not only was it impossible to establish a straight line [Fig. 3(a)] but also a positive slope obtained from the heating-rates of 20 and 40°C/min. Those for the isothermal sintering are presented in Fig. 4(a) and (b). The ΔH-values deduced for the TiO_2-excess composition are 522 ± 130 kJ/mol. A large deviation is obtained owing to data points from the low sintering temperature of 1250°C. Data from 1215°C could not be used to construct the plot because the low sintered density barely exceeding $\rho_{rel} = 80\%$ would have contributed predominantly from particle rearrangement. Those from sintering at >1320°C were not suitable either since liquid phase would have involved in the matter transport leading to densification. It therefore leaves a very narrow range of temperature in which the densification rates are useful in constructing such plots for the solid-state sintering. For BaO-excess, however, the ΔH-values lying in the range of 396 ± 16 kJ/mol are very similar. The indication is that it has been sintered by an identical mechanism.

3.2. Microstructure analysis

3.2.1. TiO_2-exess composition

Fig. 5(a) and (b) give the successive development of sintered microstructure for the 0.997 TiO_2-excess powder. Coarsening has apparently overwhelmed densification at 1215°C and sintered density increases only to reach a plateau of $\rho_{rel} \approx 83\%$ after 90 h. Sintering predominates by particle coarsening is not uncommon in ceramics. The unsinterability of undoped SiC powder even at 1900°C and coarsening of Si powder compact after heating in argon atmosphere were attributed[22] to the thermodynamic factor of the high grain-boundary energy (γ_{gb}) to solid–vapour surface-energy (γ_{sv}) ratio. The elongated plate-like grains [Fig. 5(a)] exhibiting faceting have grown preferentially along a specific crystallographic orientation which is later identified to be $\langle 111 \rangle$.[6,23–25] These grains are normally of $\sim$ 20 μm in size with an aspect ratio of $\sim$ 3–5. Single twins and double twins were both observed,[8,23–26] which are characteristic only to low temperature sintered TiO_2-excess samples. The (111) double twin plane is clearly discernible from an SEM micrograph on which the twin

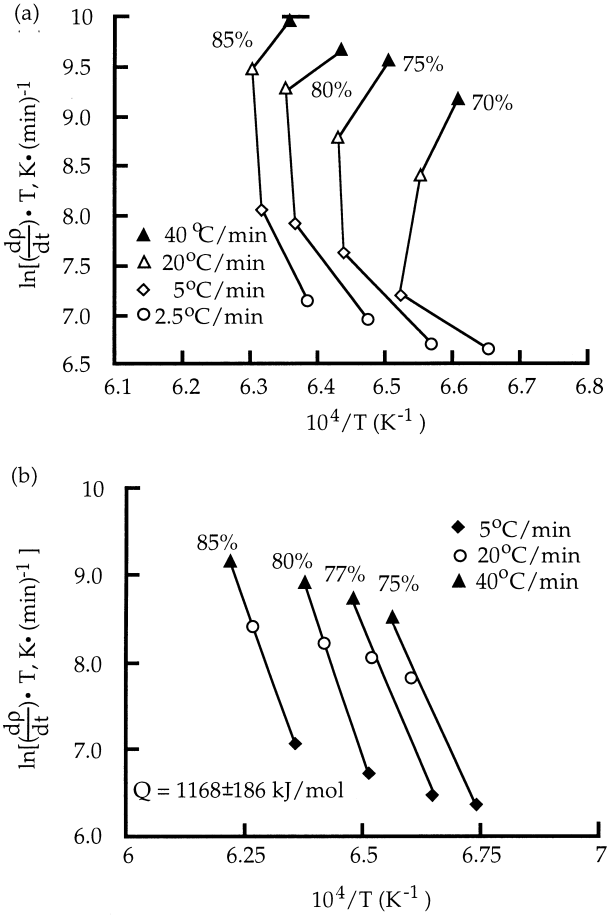

Fig. 3. Activation enthalpy values derived from constant heating-rate sintering for (a) TiO_2-excess and (b) BaO-excess composition.

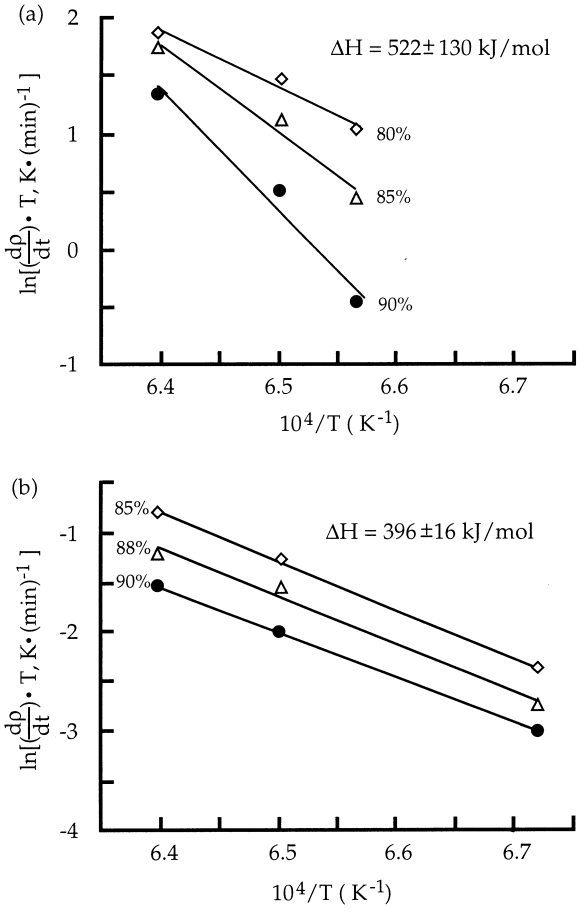

Fig. 4. Activation enthalpy values derived from the isothermal sintering kinetics for (a) TiO_2-excess and (b) BaO-excess composition.

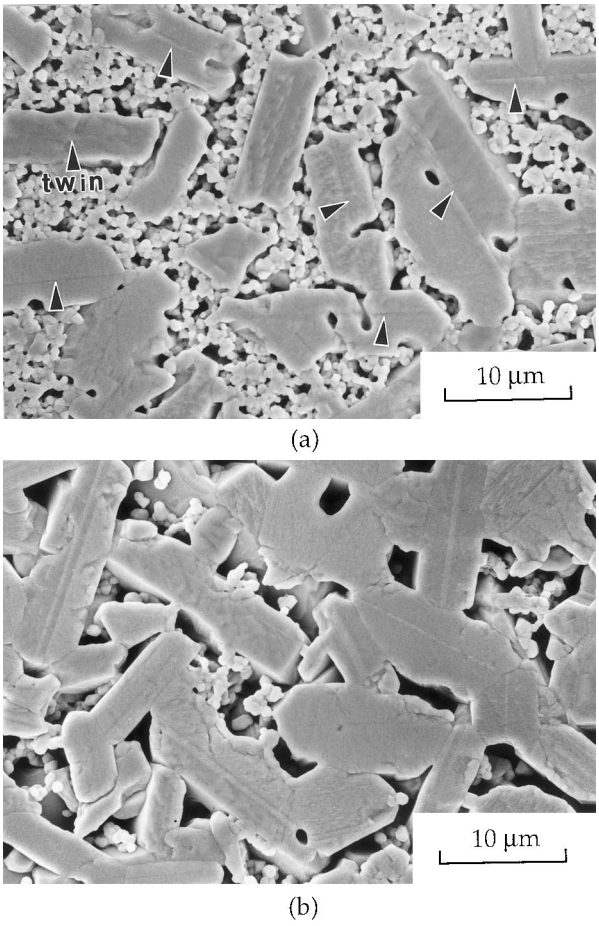

Fig. 5. Microstructure development for TiO_2-excess 0.997 composition sintered at 1215°C for (a) 20 h and (b) 55 h.

lamellae of ~ 1 μm thick lie [as indicted in Fig. 5(a)]. The sintered microstructure has evolved to the bimodal grain-size distribution [Fig. 5(a)]. The formation of these twins has also occurred in the polygonal $BaTiO_3$ grains sintered from powders prepared from the mixed-oxide route.[24]

As firing continues, the twin plate-like grains thicken laterally and grow longitudinally at the expense of the fine powder particles when the aspect ratio is retained until they gradually impinge on one another in developing to a rigid network. The bimodal grain-size distribution has lost its smaller grains [Fig. 5(b)] upon coarsening. Large plate-like grains which have grown at the expense of small ones represent Ostwald ripening in the absence of any liquid phase. It is a low ($d\rho/dG$)-ratio process in which grains grow rapidly with negligible total system shrinkage. Further densification is hindered by the skeleton of plate-like grains as they eventually develop to a rigid network. Densification is practically stopped at $\rho_{rel} \approx 83\%$ of such a skeletal microstructure [Fig. 5(b)], as can be seen from the kinetic curve (Fig. 1). Consequently, large residual pores of the triangular shape located in triple-grain junctions remain in the sintered samples [Fig. 5(b)]. Although similar abnormal grain growth has been reported[8] in the past, the corresponding kinetics is not available. It is in fact a common observation when sintered at 1215°C for an TiO_2-excess compositions of 0.900, 0.950 and 0.997 investigated here. For sintering at 1265°C/20 h, the bimodal grain structure containing $Ba_6Ti_{17}O_{40}$ which forms by solid-state reaction upon heating is clearly visible in Fig. 6(a). Faceted crystallographic planes of {111} and {100} along the interface of $Ba_6Ti_{17}O_{40}$ or polytitanates and $BaTiO_3$ [as indicated in Fig. 6(b) and the SADP inset] suggests the existence of liquid phases during sintering at 1390°C which has in fact been confirmed by lattice-fringe imaging for other samples.[6] Small $BaTiO_3$ grains exhibiting a rounded surface are also the characteristic of liquid-phase sintering. The existence of a thin glassy phase of ~ 1 nm from sintering at 1265°C/20 h is exhibited in Fig. 6(c).

The spatial density of plate-like grains (N_p) in the sintered ceramic (as counted from the SEM micrographs) against the sintering temperature is presented in Fig. 7. It shows a decreasing trend of Np with increasing sintering temperatures, e.g. from 8.8×10^8 m^{-2} at 1215°C to 7.0×10^7 m^{-2} at 1280°C. It stops increasing after sintering at 1280°C for merely 5 h when still escalating at 1215°C, even after dwelling for 96 h. The nucleation of the plate-like grains has been reduced significantly by higher sintering temperature at 1280°C which is below the $BaTiO_3$–$Ba_6Ti_{17}O_{40}$ eutectic point. Fast-firing by a heating rate of >400°C/min in a conventional tube furnace is apparently not able to suppress the coarsening mechanism, which has led to the formation of the plate-like grains. Coarsening appears to be a process of lower activation enthalpy rather than densification for the sintering of TiO_2-excess $BaTiO_3$ composition.

The plate-like grains disappear concurrently to the loss of its {111} faceting, when entering is raised to higher temperatures of 1280–1320°C[27,28] although some of the (111) double twins have been retained [Fig. 8(b)]. The characteristic faceting has been lost after annealing at 1340°C, above the $BaTiO_3$–$Ba_6Ti_{17}O_{40}$ eutectic temperature, although microfaceting changed to {100} and {111} is detected as given in Fig. 5(b). Most of the abnormally grown plate-like grains in samples sintered at 1250°C [Fig. 8(a)] become more polygonal in shape [Fig. 8(b)]. It has eventually been transformed into the typical microstructure [Fig. 8(c)] by longer annealing at 1340°C. The latter contains grain-boundary second-phases indicating liquid-phase sintering has been detected by TEM.[6]

3.2.2. BaO-excess composition

Furnace-sintered BaO-excess 1.013 samples produce the microstructure of typical polycrystalline ceramics represented by Fig. 9(a) and (b), with average grain sizes of $G_{av} = 8.0$ μm for 1215°C/100 h and $G_{av} = 20$ μm for 1290°C/100 h, respectively. Second-phase grains

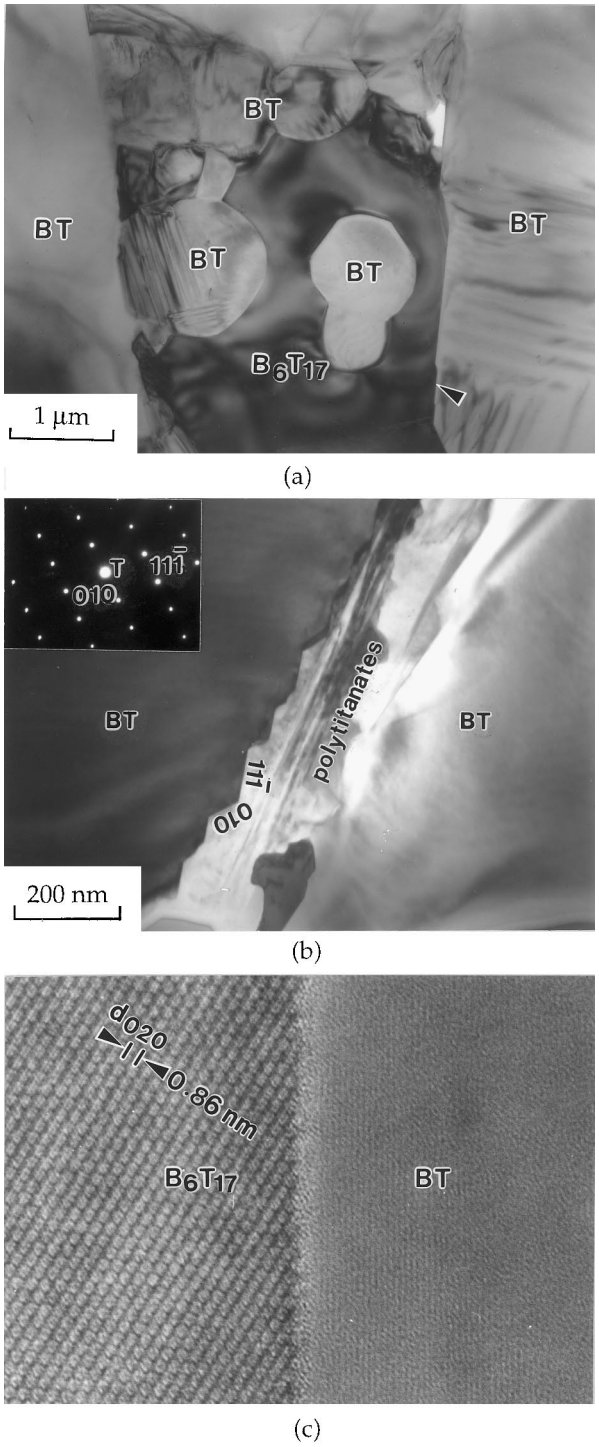

Fig. 6. Microstructure of TiO_2-excess sample sintered at 1265°C/20 h, (a) bimodal grain size containing $Ba_6Ti_{17}O_{40}$, faceted $Ba_6Ti_{17}O_{40}$-$BaTiO_3$ interface (TEM-BFI) and (b) existence of a glassy phase (TEM-LFI).

observed from hot-pressed samples[3] are not immediately discernible by SEM-SEI. A large amount of grain pull-outs in polished sections is typical in these sintered samples [Fig. 9(a)]. Previous reports[1,3] have attributed this to the highly hygroscopic phase of Ba_2TiO_4. These grains were dissolved in water during sample preparation for

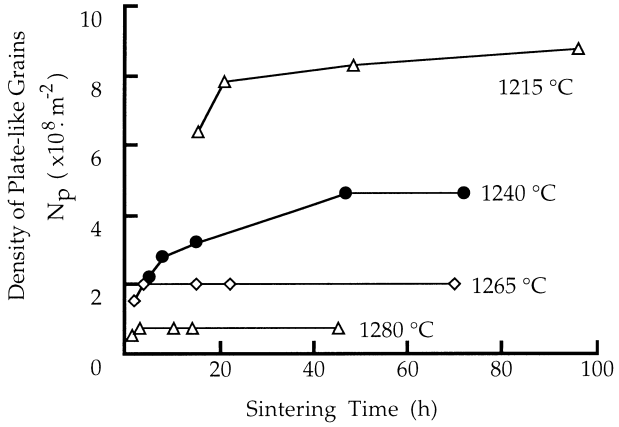

Fig. 7. The spatial density of plate-like grains (N_p) observed from samples sintered at temperatures in the range of 1215–1280°C.

microscopy when Ba_2TiO_4 reacts with water to form $Ba(OH)_2$ and was leached out subsequently.[3] The samples were very fragile, probably due to the abundant intergranular cracks [shown in Fig. 9(b)]. It is a common experience that sintered samples left in a humid atmosphere were soon found to become extremely friable upon handling. Consequently, analysis of their microstructure is rarely possible. The delineated grain boundaries appear to be cracks [Fig. 9(b) and (c)], unlike what have usually been observed of a chemically etched polycrystalline ceramic. It has usually been attributed to a more soluble grain-boundary phase by the etching solution. However, no direct evidence has been provided to confirm the existence of $Ba(OH)_2$ along the grain-boundaries of the BaO-excess samples. Residual pores intragranularly located represent the abnormal grain growth that has occurred. Ferroelectric domains are clearly visible but double twins often found in TiO_2-excess samples have not been detected.

The fracture surface of a sample sintered at 1350°C reveals abnormally grown grains with intragranular located inclusions of Ba_2TiO_4 [indicated in Fig. 9(c)] and residual pores. Fig. 10(a) presents dark-field (DF) image using $\mathbf{g}=012$ of Ba_2TiO_4, which is only found very occasionally. Considerable difficulties with foil preparation are encountered owing to its hygroscopic nature. Apparently, most of them have fallen off or dissolved in water since intragranularly located residual pores are often observed in other foils. A continuous grain-boundary phase of the glassy nature [as indicated by the diffuse ring in Fig. 10(b)] can also be discerned. Lattice fringe image of a different area in the same foil is shown in Fig. 10(c), where the glassy grain-boundary phase of $\sim$ 2 nm has been identified unambiguously. Moreover, microanalysis using AEM3010 failed to detect any elements but Ba and Ti. It is not likely to be siliceous since the minute impurity content of several hundred ppm cannot account for its continuous nature over the entire sample. Grain-boundaries consisting of

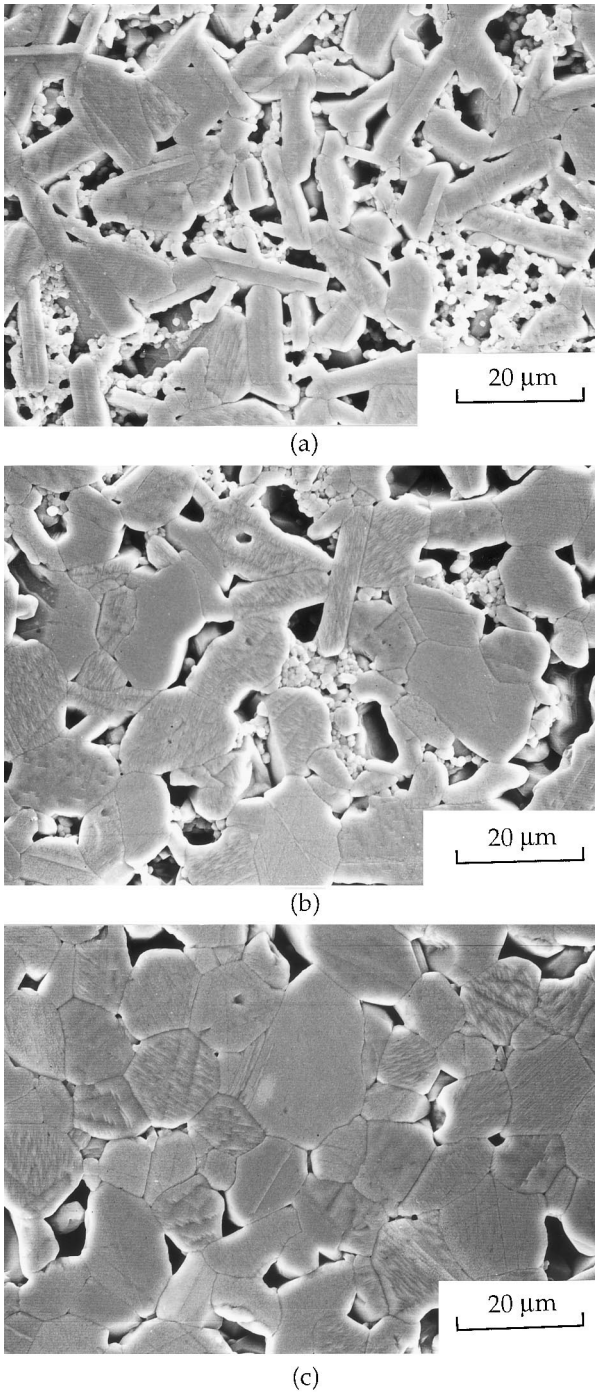

Fig. 8. Microstructure of post-sintering annealed TiO_2-excess samples of (a) sintered at 1250°C/30 h, and annealed at 1340°C for (b) 5 min and (c) 60 min.

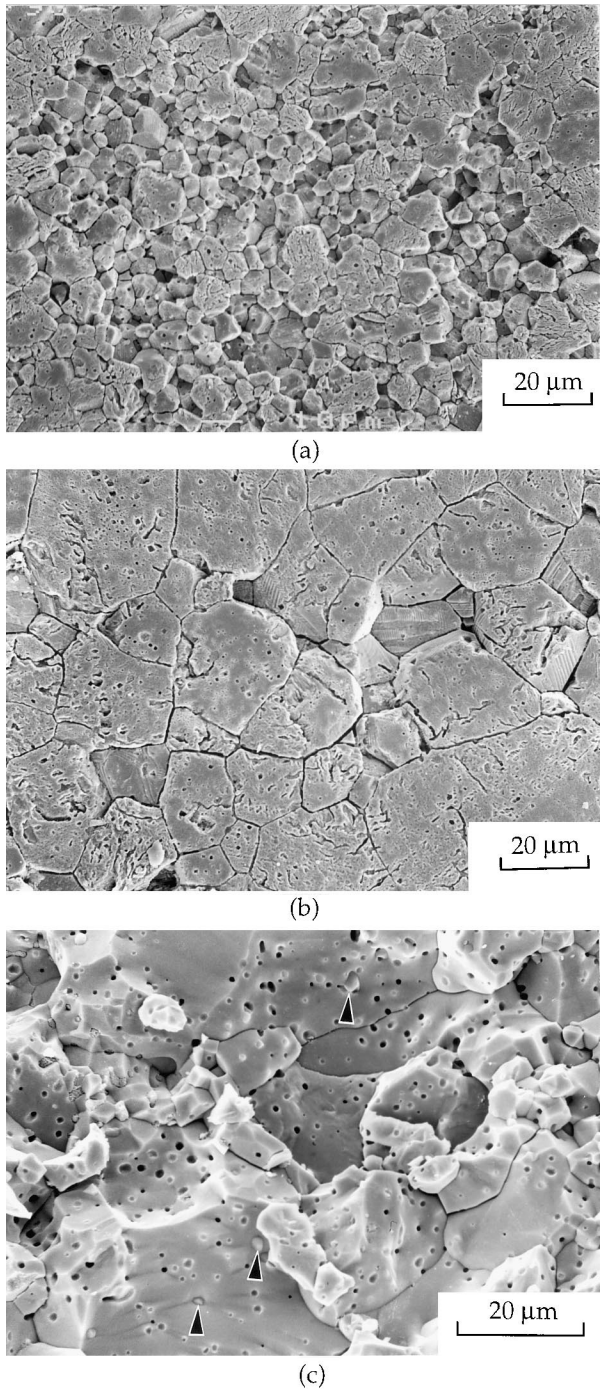

Fig. 9. Characteristic microstructure of the undoped BaO-excess samples sintered at (a) 1215, (b) 1290 and (c) 1350°C for 100 h (SEM-SEI).

BaO-rich phases (e.g. of Ba_2TiO_4) appear to have dissolved to become amorphous as observed from thin foils [Fig. 10(c)] and etched away in polished sections [Fig. 9(b)]. However, small precipitates contained in triple-grain junctions could not be identified[6] unamiguously from the selected area diffraction pattern (SADP) to substantiate the dissolution reaction of the hygroscopic Ba_2TiO_4 with water to $Ba(OH)_2$ and TiO_2.

4. Discussion

4.1. Densification mechanism

The ΔH-values depending upon the heating-rate have been reported before for pressureless-sintering of $BaTiO_3$.[14] These values, listed in Table 1 are in the range of 290 ~ 500[29] and 336 ~ 588 kJ/mol.[14] Those from the

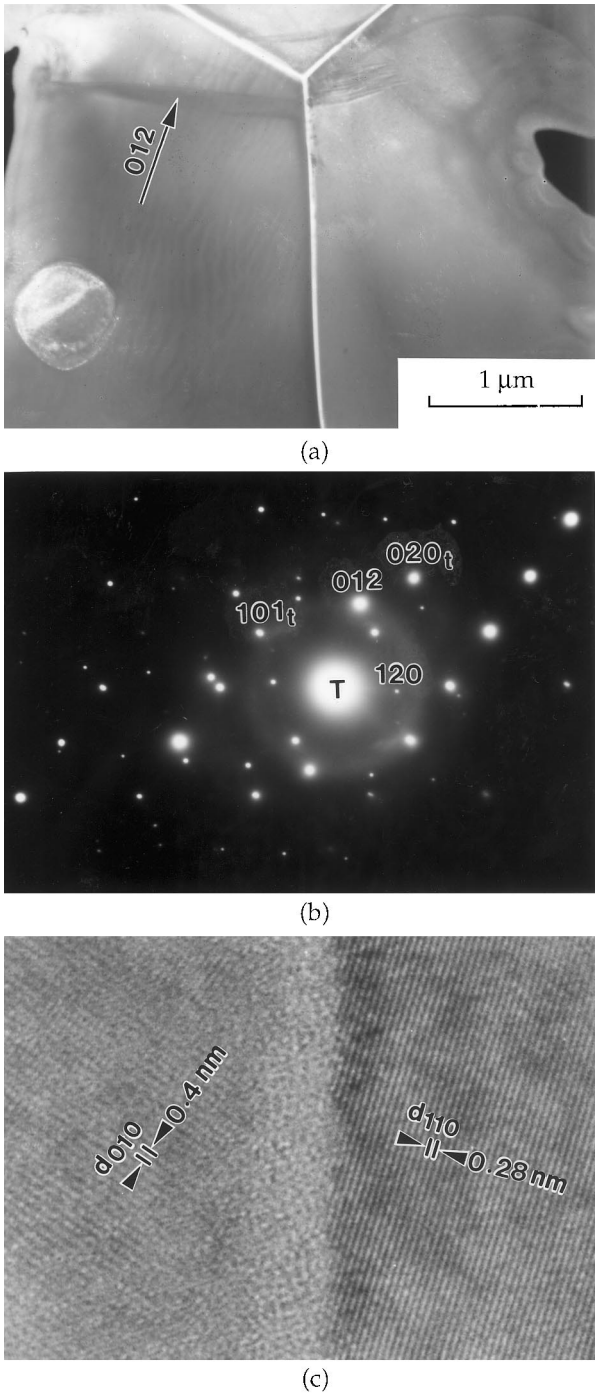

Fig. 10. TEM DF images reveal the intragranular Ba_2TiO_4 particle using (a) $\mathbf{g}=012$ of Ba_2TiO_4, (b) the corresponding SADP and (c) glassy grain-boundary phase of the continuous nature.

present study are 392, 522 and 652 kJ/mol for the TiO_2-excess composition and 380, 396 and 412 kJ/mol for the BaO-excess. Apart from the deviation of $\Delta H = 652$ kJ/mol at $\rho_{rel} = 90\%$, all of the others fall in the range of 290 $\sim$ 588 kJ/mol reported previously. Grain-size exponent from the hot-pressing technique used to identify the grain-boundary diffusion mechanism[4] was confined to a rather limited range of particle size (0.4 $\sim$ 0.9 μm) to offer its legitimacy convincingly. It appears that densification is more likely to be controlled by the lattice-diffusion of Ba^{2+} since the derived and ΔH-values are much too small in comparison with those for that of Ti^{4+} from theorectical calculation (Table 1). In particular, the ΔH of 400 kJ/mol obtained[4] from low temperature hot-pressing in the solid state (1060–1200°C) is in fact very similar to that of 396 ± 16 kJ/mol from the BaO-excess composition. Sintering by an identical mechanism can be inferred from the consistency of the activation enthalpies deduced from different degrees of densification in Fig. 4(b). Grain-boundary amorphous phase of the BaO-excess sample containing no silicon also indicates sintering has taken place in the solid state for the BaO-excess samples. Furthermore, it appears that the derived ΔH of $\sim$ 396 kJ/mol truly represents the solid-state sintering mechanism.

Higher ΔH-values from the TiO_2-excess composition is probably owing to liquid presence as that of 506 kJ/mol derived[1] from compositions containing the BaO–TiO_2 eutectic liquid and aluminosilicate glass. In fact, higher densification rates [Fig. 4(a)] obtained from sintering temperatures of >1250°C contributed by the assistance of liquid phase[20] is also suggested by the existence of a glassy grain-boundary phase shown in Fig. 6(b). The gradual increase of ΔH-values on densifying may then be attributed to the change of sintering mechanism from solid state to one of higher activation enthalpy involving liquid-phase.[1] As a result, considerable span of the and ΔH-values[14,29] derived from the sintering of TiO_2-excess compositions is expected. It can also account for the dependence of ΔH on the heating-rate adopted,[14] and, so, the anomaly from the Arrhenius plot of Fig. 3(a). Although densification is contributed predominantly by particle rearrangement for $\rho_{rel} \leqslant 80\%$, $\Delta H = 392$ kJ/mol derived [Fig. 4(a)] close to those found for the BaO-excess composition [Fig. 4(b)] indicates solid-state sintering. As temperature is raised to above 1250°C, densification is enhanced by liquid phase(s) and the activation enthalpy is increased since the predominant mechanism has altered to involve the liquid.

4.2. Coarsening

Mutual solid solubility of cations in $BaTiO_3$ is small in the range of $\sim$ 100 and 1000 ppm for BaO and TiO_2, respectively.[2,3] Consider that for the Schottky intrinsic disorder, the most probable defect structure for the BaO-excess composition may be described by,

$$BaO \rightarrow Ba^{x}_{Ba} + V''''_{Ti} + O^{x}_{O} + 2V^{\bullet\bullet}_{O} \quad (1)$$

where the titanium vacancy is the predominant cation defect. Analogously, the barium vacancy dominates the defect structure in TiO_2-excess composition and its defect reaction described by,

$$TiO_2 \rightarrow Ti^{x}_{Ti} + V''_{Ba} + 2O^{x}{}_{O} + V^{\bullet\bullet}_{O} \quad (2)$$

Better densified $BaTiO_3$ ceramic obtained from the TiO_2-excess composition is therefore expected from the solid-state sintering if the lattice-diffusion of barium is rate-determining as the ΔH values have suggested and as has been discussed previously. Nevertheless, the BaO-excess composition exhibiting better densification up to 150 h for sintering at 1215°C (Fig. 1) is just a reverse of this thought, since sintering of the TiO_2-excess composition having barium vacancy as the predominant defect species should have been encouraged in the solid state. We argue in the following from grain coarsening and offer a plausible interpretation to account for the apparent contradiction.

Plate-like faceted grains are the characteristic microstructural feature of TiO_2-excess composition (Fig. 5) sintered at a temperature of 1215°C below any possible eutectic liquid. Its growth necessitates the coalescence of grains takes place on the {111} plane which is probably of lower solid–vapour surface energy (γ_{sv}). Indeed, the planes of {111} and {100} have been reported[8] to be the low energy planes in $BaTiO_3$, and a mechanism of the (111) twin formation proposed. Coarsening predominated at lower temperatures would have occurred by mechanisms such as evaporation–condensation or surface diffusion of lower activation enthalpy encouraged preferentially by larger thermodynamic driving force for grains to grow and facet on the {111} plane. Densification contributed by particle rearrangement in the initial stage of sintering would then have led to the growth of plate-like grains sustained until later stages to develop the rigid network. Not only the low ($d\rho/dG$)-ratio has resulted to low sintered density, the rigid network thus developed has also contributed to hinder further densification, similar to what was observed in $A1_2O_3$–ZrO_2 system.[30] Densification of the TiO_2-excess samples at low temperatures of, for example, 1215°C in the solid state, although promoted by the higher concentration of barium vacancy, is surpassed by the BaO-excess. It may be attributed to the coarsening of (111) faceted grains having lower ΔH than the densification and the rigid network subsequently developed.

Grain growth along the {111} plane occurs until liquid phase forms at >1250°C. Faceting still exists [Fig. 6(a)] along the solid–liquid interface of $BaTiO_3$ grain and eutectic-liquid (of probably the Al_2O_3–SiO_2–TiO_2 composition).[6] However, liquid formation has promoted densification when coarsening occurs predominantly by evaporation–condensation but, on the other hand, densification is suppressed effectively as its matter transport path is blocked by the liquid film. Furthermore, the (solid–liquid) surface energy anisotropy has been modified by the presence of liquid eutectic to {100} and {111} [Fig. 6(b)]. The spatial density of plate-like grains decreasing with sintering temperature (Fig. 7) is evidently supportive. Therefore, it appears that the sintering of $BaTiO_3$ should benefit from fast-firing in the solid state owing to coarsening mechanisms of lower activation enthalpy. However, fast-firing in the solid state at higher temperatures has been prevented by the eutectic liquid formation at 1332°C.

The BaO-excess composition having different chemistry (of Ba_2TiO_4 or simply BaO-rich) on the grain surface would have escaped from the preferential grain growth of the TiO_2-excess samples. It is likely that the surface energy anisotropy allowing plate-like grain growth is modified to the less favourable direction when the Al_2O_3–SiO_2–TiO_2 liquid formed in the TiO_2-excess compositions is also not available. Indeed, faceting of the kind shown in Figs. 6(a) and (b) is not observed in sintered BaO-excess samples when sintered microstructure of the tetrakaidecahedral shape is typical [Fig. 9(a)]. Therefore, the BaO-excess composition may have gone through predominantly solid-state sintering and the ΔH-values derived are used to deduce the rate-determining mechanism.

5. Conclusions

The activation enthalpy values (ΔH) derived from the pressureless-sintering of the TiO_2-excess and BaO-excess compositions are 522 ± 130 and 396 ± 16 kJ/mol, respectively. Barium vacancy appears to be the rate-determining species for the solid-state sintering of $BaTiO_3$ compositions. Surface energy anisotropy may have led to the plate-like grain growth preferentially along {111} plane when sintered at low temperatures of 1215°C. Liquid-phase formation at >1250°C has resulted in the loss of faceting, better densification and development of polygonal grains.

Acknowledgements

Funding of this research by the National Science Council of Taiwan through NSC80-0405-E110-018, 82-0405-E110-029, and 83-0405-E110-007 is acknowledged.

References

1. Mostaghaci, H. and Brook, R. J., Kinetics of hot-pressing of $BaTiO_3$ ceramics. *Brit. Ceram. Trans. J.*, 1985, **84**, 203–206.
2. Sharma, R. K., Chan, N. H. and Smyth, D. M., Solubility of TiO_2 in $BaTiO_3$. *J. Am. Ceram. Soc.*, 1981, **64**(8), 448–451.
3. Hu, Y. H., Harmer, M. P. and Smyth, D. M., Solubility of BaO in $BaTiO_3$. *J. Am. Ceram. Soc.*, 1985, **68**(7), 372–376.
4. Xue, L. A., Chen, Y., Cilbart, E. and Brook, R. J., The kinetics of hot-pressing for undoped and donor-doped $BaTiO_3$ ceramics. *J. Mater. Sci.*, 1990, **25**, 1423–1428.
5. Kirby, K. W. and Wechsler, B. A., Phase relations in the barium–titanium oxide system. *J. Am. Ceram. Soc.*, 1991, **74**(8), 841–847.

6. Lin, M. H., Pressureless-sintering and microstructure development of non-stoichiometric $BaTiO_3$ compositions. Ph.D., National Sun Yat-Sen University, 1998.
7. Matsuo, Y., Fujimura, M., Sasaki, H., Hagase, K. and Hayakawa, S., Semiconducting $BaTiO_3$ with addition of Al_2O_3, SiO_2 and TiO_2. *Bull. Am. Ceram. Soc.*, 1968, **47**(3), 292–297.
8. Kastner, G., Wagner, R. and Hilarius, V., Nucleation of twin by grain coalescence during the sintering of $BaTiO_3$ ceramics. *Philos. Mag.*, 1994, **A69**(6), 1051–1071.
9. Freer, R., Bibiography self-diffusion and impurity diffusion in oxides. *J. Mater. Sci.*, 1980, **15**, 803–824.
10. Lewis, C. V. and Catlow, C. R. A., Defect studies of doped and undoped barium titanate using computer simulation techniques. *J. Phys. Chem. Solids*, 1986, **47**(1), 89–97.
11. Wernicke, R., Defect chemistry and electrical conductivity of doped barium titanate ceramics Part IV. The kinetics of equilibrium restoration in barium titanate ceramic. *Philips Res. Repts*, 1976, **31**(part 4), 526–543.
12. Anderson, H. U., Initial sintering of $BaTiO_3$ compacts. *Am. Ceram. Soc.*, 1965, **48**(3), 118–121.
13. Shirasaki, S., Yamamura, H., Haneda, H., Kakegewa, K. and Moori, J., Defect structure and oxygen diffusion in undoped and La-doped polycrystalline barium titanate. *J. Chem. Phys. Solids*, 1980, **73**(9), 4640–4645.
14. Genuist, C. and Haussonne, F. J. M., Sintering of $BaTiO_3$: Dilatometric analysis of diffusion models and microstructure control. *Ceram. Int.*, 1988, **14**, 169–179.
15. Chiang, Y. M. and Peng, C. J., Grain-boundary nonstoichiometry in spinels and titanates. In *Nonsotichiometric Compounds, Vol. 23*, ed. C. R. A. Catlow and W. C. Mackrodt. American Ceramic Society, Westerville, OH, 1987, pp. 361–377.
16. Lin, T. F., Hu, C. T. and Lin, I. N., Influence of stoichiometry on the microstructure and positive temperature coefficient of resistivity of semiconducting barium titanate ceramics. *J. Am. Ceram. Soc*, 1990, **73**(3), 531–536.
17. Chiang, Y. M. and Takagi, T., Grain-boundary chemistry of barium titanate and strontium titanate: I, high temperature equilibrium space charge. *J. Am. Ceram. Soc.*, 1990, **73**(11), 3278–3285.
18. Wu, T. B. and Lin, J. N., Transition of compensating defect mode in niobium-doped barium titanate. *J. Am. Ceram. Soc.*, 1994, **77**(3), 759–764.
19. Mendelson, M. I., Average grain size in polycrystalline ceramics. *Am. Ceram. Soc.*, 1969, **52**(8), 443–446.
20. Matsuo, Y. and Sasaki, H., Exaggerated grain growth in liquid-phase sintering of $BaTiO_3$. *J. Am. Ceram. Soc.*, 1971, **52**(9), 471.
21. Levin, E. M., Robbins, C.R. and McMurdie, H.F. BaO-TiO_2 system *Phase Diagrams for Ceramists* Vol. I. American Ceramic Society, Columbus, OH, 1964 (Fig. 564).
22. Greskovich, C. and Rosolowski, J. H., Sintering of covalent solids. *J. Am. Ceram. Soc.*, 1976, **59**(7–8), 338–343.
23. Krasevec, V., Drfenik, M. and Kolar, D., Genesis of the (111) twin in barium titanate. *J. Am. Ceram. Soc*, 1990, **173**(4), 856–860.
24. Oppolzer, H. and Schmelz, H., Investigation of twin lamellae in $BaTiO_3$ ceramics. *Am. Ceram. Soc.*, 1983, **66**(6), 44–46.
25. Eibl, O., Pongeratz, P. and Skalicky, R., Crystallography of (111) twins in $BaTiO_3$. *Philos. Mag.*, 1988, **B57**(4), 521–534.
26. Recnik, A., Bruley, J., Mader, W, Kolar, D. and Ruhle, M., Structural and spectroscopic investigation of (111) twins in barium titanate. *Philos. Mag.*, 1994, **B70**(5), 1021–1034.
27. Hennings, D. F. K., Janssen, R. and Reynen, P. J. L., Control of liquid-phase-enhanced discontinuous grain growth in barium titanate. *Am. Ceram. Soc.*, 1987, **70**(1), 23–27.
28. Xue, L. A. and Brook, R. J., Promotion of densification by abnormal grain growth. *Am. Ceram. Soc.*, 1989, **72**(2), 341–344.
29. Enomoto, Y. and Yamaji, A., Preparation of uniformly small-grained $BaTiO_3$. *Am. Ceram. Soc. Bull.*, 1981, **60**(5), 566–570.
30. Sudre, O. and Lange, F. F., Effect of inclusions on densification: I, Microstructural development in an Al_2O_3 matrix containing a high volume fraction of ZrO_2 inclusions. *Am. Ceram. Soc.*, 1992, **75**(3), 519–524.